Journal of Coastal Research	17	2	420–430	West Palm Beach, Florida	Spring 2001

Predicting the Depth, Across-Channel Location, and Speed Variability of Tidal Current Core Maxima at the Mouth of the Chesapeake Bay

Dennis J. Whitford

Department of Oceanography
572M Holloway Road
U.S. Naval Academy
Annapolis, MD 21402 U.S.A.

ABSTRACT

WHITFORD, D.J., 2001. Predicting the Depth, Across-Channel Location, and Speed Variability of Tidal Current Core Maxima at the Mouth of the Chesapeake Bay. *Journal of Coastal Research*, 17(2), 420–430. West Palm Beach (Florida), ISSN 0749-0208.

Reasonable prediction of the depth, across-channel location, and speed variability of tidal current core maxima at the mouth of the Chesapeake Bay can be determined to first order without an extensive deployment of current meters. Fourteen tidal current data sets were acquired with a shipboard Acoustic Doppler Current Profiler (ADCP) on track lines across the Bay mouth. Data sets were representative of fortnightly tidal range variation (spring, neap, and transitional), as well as semi-diurnal tidal current cycle phases (ebb, flood, and slack) for the months of June and September in four different years. Data indicated tidal current maxima were contained within a narrow jet-like core with a horizontal scale of O(1–2 km) and vertical scale of O(10 m). The depth, across-channel location, and speed of the maxima varied with the semi-diurnal tidal current cycle phase, and to a much lesser extent, with the fortnightly variation of tidal range. This temporal variability is modeled by least squares using a sinusoidal function, related to the dominant tidal current harmonic constituent, and a third-degree polynomial curve fit. Prediction algorithms from both models result in correlation coefficients for depth (0.95), across-channel location (0.97), and speed (0.93). National Oceanic and Atmospheric Administration (NOAA) tidal current tables had a speed correlation coefficient of only 0.79 when matched to observations. Comparison correlation coefficients for depth and across-channel location from NOAA tidal current tables could not be determined since the tables do not provide this information. This method provides a first-order, empirical means for predicting the depth, across-channel location, and speed variability of tidal current core maxima under conditions of similar atmospheric forcing and freshwater input without long-term deployment of current meters at multiple depths and locations. The method is not site-specific. Therefore, it may be applied at other locations and could be especially beneficial to estuaries where there are no tidal current meters or published tidal current information.

ADDITIONAL INDEX WORDS: *Acoustic Doppler Current Profiler (ADCP), estuaries, current meter.*

INTRODUCTION

Comprehensive knowledge of tidal currents is essential for safe navigation, coastal and oceanic engineering, contaminant disposal, effective military operations, and management of estuarine ecosystems. Knowledge of estuary currents is essential to understanding material fluxes into and out of the estuary. These fluxes have a direct effect on estuarine life cycles and water quality (VALLE-LEVINSON, 1998). Yet for many of the world's estuaries, there is minimal or no detailed tidal current data available. Even in the United States, tidal current tables only provide general information, and are often based on decades-old current meter data (50% of the U.S. tidal current stations listed in the National Oceanic and Atmospheric Administration's (NOAA's) Tidal Current Tables predate 1970) with coarse spatial resolution (O[10^4 m]) and short duration (60% of U.S. tidal current stations listed in the Tidal Current Tables are based on a survey length of less than 15 days) (EHRET and KENDRICK, 1999). Therefore accurate prediction of tidal currents, without the use of current meters, would be valuable.

Data documenting the rise and fall of water level in response to tidal forcing is adequately acquired from the many operating tide stations located around the world. To a first-order approximation, tidal level values acquired nearshore (*e.g.* from a pier) represent water elevation along the coastline and offshore from the station. Tidal height analysis and prediction is commonplace using this data.

Unfortunately, tidal current analysis and prediction is much more difficult. The cost of deploying a current meter is from four to ten times as expensive as deploying equipment to measure water level. Continuous water level observation has occurred at some locations since the mid 1800s; whereas continuous current observations began only a few years ago. Compared to tide stations, there are relatively few operating tidal current stations. Most tidal current stations have significantly less spatial resolution to describe a more spatially varying phenomena, and many of them have been active for only a short period of time. Hence most tidal current predic-

99088 received 8 October 1999; accepted in revision 17 September 2000.

tions, when there are any, are mathematically inferred from limited duration data often taken decades ago.

Unlike water level, tidal currents vary spatially in three dimensions to a first order approximation. At an estuary mouth, one would need many current meters placed at multiple depths and locations to provide the same level of coverage as one or two tide level stations. Thus, an individual seeking detailed tidal current information must seek local mariners whose experience in the area, both fortunate and unfortunate, may provide some anecdotal information regarding the spatial and temporal variability of local tidal currents.

Within any tidal current regime, there is a maximum current usually embedded within a narrowly defined core of current flow. Knowledge of the spatial and temporal distribution of this jet maximum would be important for those wishing to avoid, or take advantage of, its properties. Mariners navigating a channel, engineers designing a pipeline crossing or submerged structure, and military forces wishing to covertly enter and exit an estuary would benefit from comprehensive knowledge of the depth, across-channel location, and speed variability of tidal current core maxima.

Factors affecting the spatial and temporal variability of tidal current core maxima include earth's rotation, atmospheric pressure, wind stress, bathymetric variations, water density gradient, estuarine type, freshwater input, and fortnightly variability in tidal range. Although most previous work has addressed subtidal flow (also known as residual or mean flow), there is some information regarding the tidally-aliased core flow, which is the subject of the paper.

Focusing on the main channel of the Chesapeake Bay mouth, WHITFORD (1999) found tidal currents to have a classical gravitational circulation modified by coriolis with a near surface (and less dense) ebb current and a subsurface (and more dense) flood current, both to the right of flow direction. This tendency is explained by OFFICER (1976) and OPEN UNIVERSITY COURSE TEAM (1989) among others.

Increased fresh water outflow from geologic springs, as well as increased precipitation, would increase ebb flow due to volume considerations. This would be especially true in highly stratified and partially mixed estuaries (DYER, 1997) and in smaller estuaries where the freshwater input forms a substantial part of the volume outflow. And, from general tidal theory, greater inflow and outflow would be expected during periods of large tidal range (spring tides) with reduced inflows and outflows during periods of small tidal range (neap tides).

Wind can affect the temporal variability of the velocity core. An out-of-the-estuary wind would obviously enhance the surface outflow. A strong into-the-estuary wind has even be seen to reverse a classic gravitational flow by forcing inflow at the surface and outflow near the bottom (ELLIOTT, 1978). Wide estuaries would be more influenced by wind than narrow estuaries. WANG and ELLIOTT (1978) and WANG (1979) found that the lower Chesapeake Bay responded barotropically to local winds and coastal Ekman flux producing volume exchanges larger than those produced by just estuarine circulation and freshwater discharge. And, as might be expected, there was a seasonal dependence on the wind's barotropic influence on estuaries with maximum influence being in the winter due to higher wind speeds. PARASO and VALLE-LEVINSON (1996) in a study of the lower Chesapeake Bay found that barometric pressure changes typically were less influential than wind stress on an estuarine circulation.

LI and VALLE-LEVINSON (1999) developed a numeric model for narrow estuaries, defined as narrower than the barotropic Rossby radius, and found the largest amplitude of the along-estuary tidal flow to be in deeper water. The flow rate was also influenced by the rate of change of depth with steeper channel slope correlating with maximum amplitude of the flow. These conclusions were subsequently supported by a 60-day observation of water surface elevation in the James River estuary.

Along- and across-estuary density gradients can also create density-driven current flows. VALLE-LEVINSON *et al.* (1999) discuss the complex interaction of density-driven and tidally-driven subtidal flow for the James River estuary. Along-estuary flow was found to depend on lateral depth variation and fresh water river discharge.

Thus there are several flow constituents in estuaries which interact in a very complicated fashion. However, it is not the intent of this paper to identify and focus on the relative contributions of the tidally-driven, density-driven, and meteorologically-driven flow components, but to show a simple, first-order, predictable relation to their combined result under near steady state conditions.

This paper describes a simple, first-order, empirical method to predict the depth, across-channel location, and speed of tidal current jet core maxima based solely on multiple across-channel Acoustic Doppler Current Profiler (ADCP) transects. The topic is important because many of the world's estuaries are not described by tidal current tables; and for those which are, these tables do not provide this specificity of information.

STUDY AREA

The Chesapeake Bay is one of the most studied estuaries in the world with multiple government, academic and industrial institutions focusing on it. NOAA maintains many more tide stations (18) and publishes much more tidal current information for this estuary as compared to the information promulgated for the vast majority of estuaries in the world. Yet even in this data-rich environment, tidal current coverage is poor. There are no active current meters operating in the Bay today. As part of a major scientific effort, an extensive array of tidal current meters were employed during a Bay-wide tide and tidal current survey conducted from August 1981 to December 1983 by the National Ocean Service (NOS). However the majority of these deployments were short-term (1–2 months). It is from these deployments that NOAA's annual tidal current tables are developed to provide predicted current velocities. Tidal current accuracy is not nearly as good as that for water level. This degradation in accuracy is warned by the statements "Mariners should use extreme caution and discretion in the use of published NOS tidal current predictions for this area" (NOAA, 1999a, p. XI) found in the Tables for the Hampton Roads and Thimble Shoals areas of the Bay. Because of the more robust tidal

Table 1. *Tidal current meters placed across the Chesapeake Bay mouth during the 1981–1983 National Ocean Service tidal current survey (from FISHER, 1986; NOAA, 1995).*

Cm #[1]	Sub Sta #[2]	Location Lat (N)	Location Long (W)	Depth at MLW (m)	Begin Series (date)	Series Length (days)	Harmonic Analysis (days)
38	4516	37–03.37	75–58.33	10.1	5/12/82	22	15
39	4461	07–01.40	75–59.55	6.0	5/12/82	34	29
40	4451	36–58.77	75–59.98	12.7	3/29/82	330	330 & 29[3]
41	4446	36–57.53	76–00.68	18.7	5/12/82	34	29
42	4441	36–56.33	75–59.98	14.0	5/12/82	22	15

[1] Current meter number as assigned during the 1981–1983 National Ocean Service survey.
[2] Subordinate station number as listed in NOAA Tidal Current Tables.
[3] Harmonic analysis of 29 day series beginning 12/17/83 is most representative of 330-day period.

elevation network, a similar warning is not found in the companion Tide Tables. In addition, NOAA (1999a, p. VIII) is undertaking a major quality assurance study of tidal current predictions because they ". . . do not have the funding, personnel, and other resources to verify or update tidal current subordinate stations." This action may result in removal of more than 50% of tidal current subordinate stations listed in the Tidal Current Tables.

This paper will focus on the current variability of the maximum tidal current flow in the main navigational channel of the Chesapeake Bay mouth, the Chesapeake Channel, because most of the Bay mouth's volume exchange takes place in channels (VALLE-LEVINSON *et al.,* 1998) and tidal flow amplitudes are greater in channels than over shoals (ONG *et al.,* 1994; VALLE-LEVINSON and LWIZA, 1997), especially for the Chesapeake Channel (BOICOURT, 1981). The Chesapeake Channel is also where this study identified the maximum tidal current flow for the Bay mouth. The Bay mouth had a string of five tidal current meters placed across-channel in the 1981–1983 survey (BOICOURT, 1981). Their location, date, duration, and other specifications are listed in Table 1 with specific locations illustrated in Figure 1. This is substantially more tidal current spatial coverage than is available for most other estuary mouths.

Early across-channel studies of estuarine flow employed moored current meters providing continuous temporal records but low-resolution horizontal spatial coverage (O[km]) and only a single current data point in the vertical (*e.g.* DOYLE and WILSON, 1978). This approach necessitated significant interpolation of data between moorings and provided no vertical variability information. Using these procedures, BOICOURT (1981) identified current maxima with related cores. With the recent introduction of the ADCP into estuarine studies, much higher resolution (horizontal (O[10 m to 10^2 m]) and vertical (O[1 m])) spatial coverage of flow has been obtained by several researchers (VENNELL, 1994; ONG *et al.,* 1994; VALLE-LEVINSON *et al.,* 1998; WHITFORD, 1999).

Previous studies of the Bay mouth provided an increasing

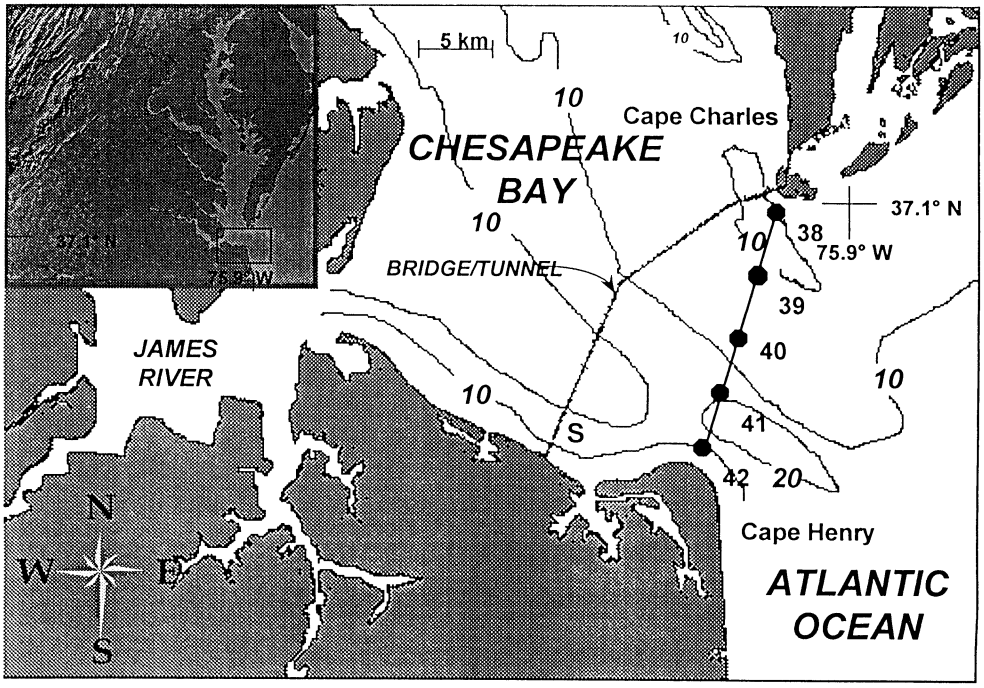

Figure 1. The mouth of the Chesapeake Bay. Contours are in meters. The straight line is the ship's Acoustic Doppler Current Profiler (ADCP) track with superimposed circles and adjacent numbers 38–42 denoting the approximate locations and array numbers of the National Ocean Service's 1981–1983 current meter array used to predict current speeds in subsequent NOAA tidal current tables. Water level and meteorological data were obtained from sensors located at the "S" alongside the Bridge/Tunnel. Map redrawn from RICHARDS and GRANAT (1986). Satellite image insert from Johns Hopkins University Applied Physics Laboratory.

Table 2. *Acoustic Doppler Current Profiler specifications.*

Parameter	Value
Manufacturer	RD Instruments
Acoustic Frequency	1200 kHz
Bandwidth	narrow
Acquisition mode	bottom track
Beam angle	30°
Vertical cell length	1 m
Sampling interval	10 s
Horizonal averaging	55 m (achieved in post-processing)
Standard deviation	0.01 ms $^{-1}$ (RD INSTRUMENTS, 1991)
Short-term random error	±0.02 ms $^{-1}$ (RD INSTRUMENTS, 2000)
Navigation	global positioning system and gyro compass

amount of tidal current specificity. BOICOURT (1981) used eleven vertical arrays of fixed current meters, horizontally spaced O(km) apart, to generalize a surface outflow and subsurface inflow in the Chesapeake Channel. GOODRICH (1987) used fixed current meters to suggest that mean flow features were relatively stable and that strong flow into the Bay was confined to the deep Chesapeake Channel. He also determined that strong outflow appeared near the surface off Cape Henry. VALLE-LEVINSON and LWIZA (1995) introduced higher resolution ADCP surveys to the southern Chesapeake Bay at a location 20 km inside the Bay mouth. They related flow structure to the hydrographic structure (VALLE-LEVINSON and LWIZA, 1997) and determined that the tidal variability was dominated by the semi-diurnal tidal constituents which displayed the greatest amplitudes and phase lags near the surface and in the North and Chesapeake Channels (VALLE-LEVINSON *et al.,* 1998). WHITFORD (1999) used high-resolution ADCP coverage to identify a consistent subsurface flood current core and a surface ebb core, both on the right side of the Bay mouth's Chesapeake Channel in the direction of flow. Prior to WHITFORD (1999), there is little discussion of the spatial and temporal variability of tidal current core maxima in any estuary. This study shows that high-resolution tidal current core variability can be predicted with just a few ADCP transects of the Bay mouth.

Table 4. *Data Analysis Groups*

Group I:	first five transects; 16–19 Sep 1996
Group II:	all fourteen transects
Group III:	all fourteen transects minus one outlier data set

METHOD

Multiple across-channel transects of the Chesapeake Bay mouth were accomplished during the months of September 1996 and June 1997, 1999, and 2000, using the U.S. Naval Academy's 102-foot oceanographic research vessel. Current data were obtained by continuous ADCP operation in one direction followed by acquisition of Conductivity-Temperature-Depth (CTD) data at seven equally-spaced locations on the return transect. WHITFORD (1999) discusses the temperature, salinity, and density structure of the Bay mouth as determined from the 1996 and 1997 data sets.

Meteorological and water level data were acquired from NOAA tide station #8638863, mounted on the Chesapeake Bay Bridge Tunnel, located 8 km to the west of the transect (Figure 1).

The ADCP used in this study was a vessel-mounted, narrowband 1200 kHz ADCP. It was operated continuously along a transect and in the bottom tracking mode so that ship motion over the bottom is removed from the sensed velocities. ADCP specifications are provided in Table 2. Acquisition horizontal averaging was approximately 25 m. The horizontal averaging of 55 m was achieved in post-processing of the data. This reduced the velocity error to ± 0.02 ms $^{-1}$ per RDI (2000).

With the sensor mounted on the vessel's hull bottom, ADCP profiles of data began at a depth of 3 m and continued to a depth equal to an advertised 85% of the total water column depth (due to acoustic interference from the bottom). ADCP data were initially displayed using RD Instruments' Transect© software. Data were then transformed into ASCII format and transferred to a spreadsheet program for subsequent manipulation by Noesys' Transform© software pack-

Table 3. *Data table. Note that generic relative times of 3.1 and 9.3 hours correspond to ebb and flood conditions respectively.*

Date	Transect#	Tidal Current Phase	Generic Relative Time (hr)	Spring (S) Neap (N) Variation	Observed Tidal Range (m)	Wind Speed (ms $^{-1}$)	Wind Direction (deg true)	Along-Strait Wnd Spd (ms $^{-1}$)	Atmos. Press (mb)	Monthly Freshwater Input (m^3s^{-1})	Volume Transport (10^3 m^3s^{-1})
16-Sep-96	16-4	slack	0.0	S–4–>N	0.814	2.6	190	−0	1016.2	−2830	20.2
18-Sep-96	18-2	sl–1.4h–>E	1.4	S–6–>N	0.895	7.7	306	7	1011.2	−2830	28.4
20-Sep-96	20-1	sl–2.9h–>E	2.9	Neap	0.597	5.1	275	5	1014.0	−2830	−59.7
16-Sep-96	16-9	E–0.8h–>sl	3.9	S–4–>N	0.846	3.9	155	−2	1015.1	−2830	−87.9
06-Jun-99	6-22	E–0.8h–>sl	3.9	Neap	0.854	3.7	71	−3	1024.4	−1274	−96.9
21-Sep-96	21-1	E–0.9h–>sl	4.0	N–1–>S	0.564	6	188	−0	1016.9	−2830	−99.9
19-Sep-96	19-2	E–1.0h–>sl	4.1	S–7–>N	0.644	9.4	334	6	1011.3	−2830	−64.8
02-Jun-00	2-2	E–1.1h–>sl	4.2	Spring	1.002	2.9	110	−3	1014.6	−2169	−47.8
01-Jun-97	1-14	E–1.4h–>sl	4.5	N–3–>S	0.842	2	103	−2	1010.3	−1726	−40.2
20-Sep-96	20-14	E–2.7h–>sl	5.8	Neap	0.734	3.8	329	2	1017.0	−2830	62.7
19-Sep-96	19-3	sl–0.9h–>F	7.1	S–7–>N	0.644	8.4	327	6	1011.9	−2830	2.5
01-Jun-97	1-15	sl–1.1h–>F	7.3	N–3–>S	0.842	4.8	89	−5	1009.5	−1726	69.6
01-Jun-97	1-17	sl–1.8h–>F	8.0	N–3–>S	1.004	5.8	85	−6	1009.3	−1726	103.8
06-Jun-99	6-23	F–0.6h–>sl	9.9	Neap	0.692	3	76	−3	1026.1	−1274	50.1
16-Sep-96	16-4	slack	12.4	S–4–>N	0.814	2.6	190	−0	1016.2	−2830	20.1

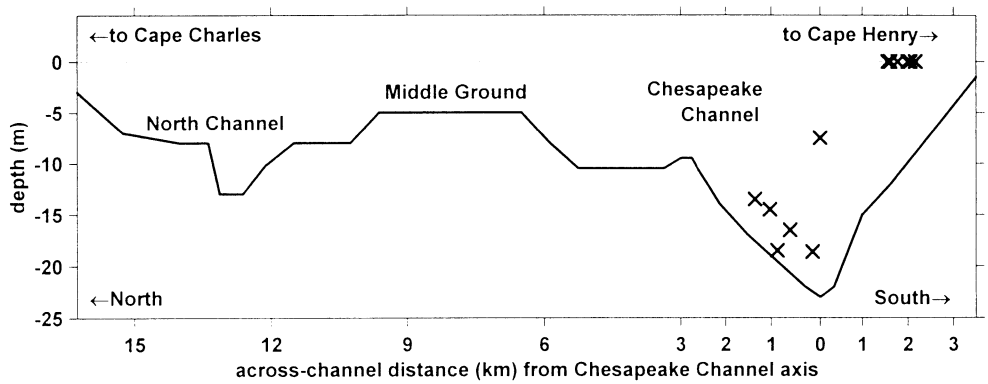

Figure 2. Across-channel bathymetric profile of the Chesapeake Bay mouth. The eleven data marks ("x") depict the spatial variability of tidal current core maxima based on this experiment's data sets. Note that there are six data points overlayed on each other at the surface between 1.5×10^3 m to 2.0×10^3 m south of the Chesapeake Channel axis.

age. Small data gaps and outliers were discarded and linearly interpolated data were substituted. Data were linearly extrapolated upward to address the inherent loss of ADCP data in the upper 3 m. Subsequent mathematical manipulation was accomplished using The MathWorks' MATLAB© software.

Fourteen transects were used in this study based on data fidelity. Data were acquired during the periods September 16–21, 1996; June 1, 1997; June 6, 1999; and June 2, 2000. Data were acquired during spring, neap, and transitional tidal ranges, as well as during all phases of a semi-diurnal tidal current cycle (Table 3). Data were acquired during periods of relatively steady-state freshwater input and atmospheric forcing. ADCP transect numbering consisted of the date, a hyphen, and the transect number of that day (*e.g.* transect 16–9 was transect number 9 acquired on September 16, 1996). This numbering system is used in several Figures.

Since the desired tidal current algorithms must be predictive, a generic tidal cycle period of 12.4 hours was selected because of the dominance of the M_2 tidal current constituent in this area (BROWNE and FISHER, 1988). Observations and predictions are referenced to this relative cycle. The observation time was selected as the time when the vessel passed directly over the Chesapeake Channel's longitudinal axis. This time was then converted to a time relative to the M_2 cycle since slack, flood, and ebb conditions are adequately inferred from the tidal current tables. For example, relative times of 0.0, 6.2, and 12.4 hours refer to slack water conditions prior to maximum ebb, flood, and ebb conditions, respectively. Relative times of 3.1 and 9.3 hours refer to maximum ebb and flood conditions respectively. This conversion could also be accomplished, if no tables were available, through direct observation of the tidal current flow.

Table 5. *Tide and tidal current harmonic constituents for the mouth of the Chesapeake Bay (NOAA, 1997). Tidal information was taken from NOAA tide station #8638863 mounted on the Chesapeake Bay Bridge Tunnel. Tidal current information was taken from a 1982 330-day temporary current meter located at 36°58′77′N 75°59′98′W and identified as station #40 in Figure 1.*

	Tide		Current			
			Major Axis		Minor Axis	
Constituent	Amplitude (m)	Phase (deg)	Speed (ms^{-1})	Phase (deg)	Speed (ms^{-1})	Phase (deg)
M_2	0.393	235.8	0.499	243.4	0.048	210.0
N_2	0.089	220.0	0.124	218.6	0.015	216.4
S_2	0.074	257.2	0.106	254.7	0.003	317.8
K_1	0.059	111.1	0.069	114.0	0.004	294.0
O_1	0.047	136.8	0.054	136.1	0.006	028.6

Wind and atmospheric pressure can influence water level and tidal currents. Their relative contribution to water level variation was analyzed using the method of PARASO and VALLE-LEVINSON (1996). Water level variation due to a change in atmospheric pressure was calculated using the inverted barometric effect:

$$\Delta\eta_{pred} = -(1/g\rho)\,\Delta p_{obs} \quad (1)$$

where $\Delta\eta_{pred}$ is the predicted change in water level, g is gravitational acceleration, ρ is water density, and p_{obs} is the observed atmospheric pressure measured in Pascals. Along- and across-channel wind component contribution to water level variation was determined from:

$$\Delta\eta_{pred} = \tau_{sx}\Delta x/(g\rho[h + \eta_{obs}]) \quad (2)$$

$$\Delta\eta_{pred} = \tau_{sy}\Delta y/(g\rho[h + \eta_{obs}]) \quad (3)$$

where τ_{sx} and τ_{sy} are the along- and across-channel wind stress components, Δx and Δy are distances over which the wind is blowing in the along- and across-channel directions, h is water depth, and η_{obs} is the observed water level.

Freshwater input can influence water level and tidal currents. Increasing freshwater input to an estuary could result in an increased ebb flow as well as asymmetry between the ebb and flood current with regard to core depth, across-channel location, and speed. In smaller estuaries, freshwater input can even overwhelm the tidal current and dominate flow throughout the tidal cycle. In that situation, the flow might not exhibit tidal periodicities but could still be modeled under steady state conditions. For the Chesapeake Bay in June and

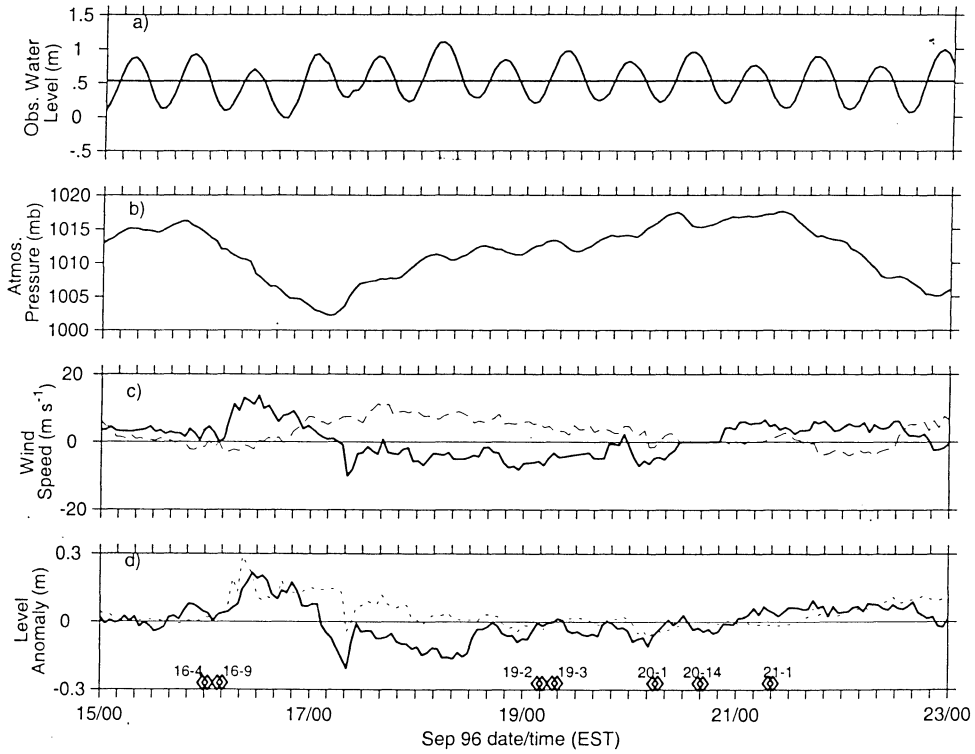

Figure 3. (a) Observed water level, (b) atmospheric pressure, (c) across- (solid line) and along-channel (dashed line) wind speed, and (d) observed water level anomaly (solid line) and water level anomaly attributed to wind stress and atmospheric pressure (dashed line) for an eight-day period bracketing the September 1996 data set. Acoustic Doppler Current Profiler transect name and duration are depicted in the lower plot. Diamond symbols denote start and stop time of each transect.

September, freshwater input comprises about 10% of the total Bay discharge into the ocean (Table 3), and thus is not a major factor in this analysis.

The transects were divided chronologically into three groups for analysis (Table 4). Group I consisted of the first five transects. They occurred during a slack-to-neap transition in tidal range and provided the data from which prediction algorithms would be initially developed. Group II, consisting of all fourteen transects, and Group III, consisting of all fourteen transects minus one data outlier, served as observations to verify the predictive algorithms developed from Group I's data.

Using observed data of depth, across-channel location, and speed of tidal current core maxima, two curve fitting methods were used to develop predictive equations. These were a third-degree polynomial fit and a sinusoidal function fit using least-squares. The polynomial fit was calculated using a MATLAB subroutine. The sinusoidal fit (SPIEGEL, 1975) is based on:

$$y = a_0 + bx \tag{4}$$

where

y = parameter to be predicted
(*i.e.* depth, across-channel location, or speed),

$$a_0 = \left[\left(\sum y\right)\left(\sum x^2\right) - \left(\sum x\right)\left(\sum xy\right)\right] \Big/ \left[n \sum x^2 - \left(\sum x\right)^2\right],$$

$$b = \left[n \sum xy - \left(\sum x\right)\left(\sum y\right)\right] \Big/ \left[n \sum x^2 - \left(\sum x\right)^2\right],$$

n = number of data points, and
x = sin[(2π/T)t],

where T is the period of the main harmonic constituent, and t is the relative time referred to a generic tidal current cycle.

RESULTS AND DISCUSSION

Data were acquired across the mouth of the Chesapeake Bay (Figure 1). The Bay mouth has a 18 km width versus a maximum width of approximately 45 km inside the bay, and has a 25 m maximum depth versus an average depth of 10 m inside the bay. The Bay mouth has several significant bathymetric features which are (listed from north to south): the North Channel of 13 m depth which does not substantially connect at depth to the Bay or Ocean; the Middle Ground which is a 3 to 4 km wide shoal area of 5 m depth; a narrow 1 to 2 km wide channel of 12 m depth; a narrow shoal area of 8 m depth; and the main Chesapeake Channel of 5 to 7 km width and 23 m depth. These features are depicted in Figure 2. The dominant harmonic constituent for

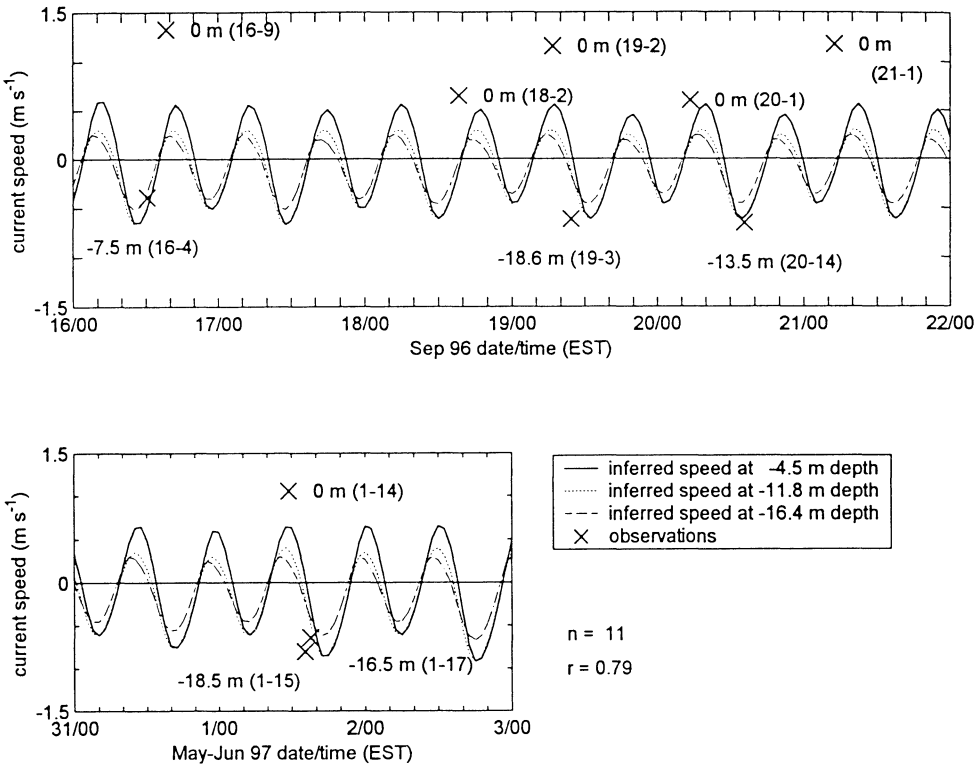

Figure 4. NOAA inferred tidal current speeds (curves) at three different depths for the Chesapeake Channel plotted against observations (X's) of tidal current core maxima for September 16–22, 1996 and May 31–June 3, 1997. Observation depths and transect numbers are annotated next to the observation marker. Correlation coefficient (r) and number of observations (n) are annotated on the graph.

tidal currents is the principal lunar semi-diurnal constituent, M_2, which has a 12.4 hr period. The largest five tide and tidal current harmonic constituents for the Bay mouth are listed in Table 5.

Data indicated tidal current maxima were contained within a narrow jet-like core with a horizontal scale of O(1–2 km) and vertical scale of O(10 m). WHITFORD (1999) illustrates these current cores in color. Depth, across-channel location, and speed of tidal current maxima were identified from each of the data sets. The Bay mouth's maximum speed always occurred in the Chesapeake Channel (Figure 2).

For the period of 15–23 September 1996, a tidal range [Figure (3a)] of less than 1 m was observed, along with an atmospheric pressure range [Figure (3b)] of 18 mb. Along- and across-channel wind components were computed (Figure 3c). Results using Equations (1) to (3) indicated that atmospheric pressure and wind accounted for most of the water level anomaly and can be visually correlated (Figure 3d). Low wind speeds were mostly prevalent during data acquisition and thus the ratio of water level anomaly to average depth was very small $O(10^{-3})$. Water level anomaly was less than $\pm$ 0.3 m [Figure 3(d)] for the eight-day period and was less than $\pm$ 0.05 m for the times of the ADCP transects themselves. Thus, atmospheric pressure and wind were not considered factors in affecting tidal currents during this period. The meteorological conditions, tidal range, and freshwater input for this period were representative for all periods of data acquisition.

To assess the accuracy of NOAA's predicted tidal current speeds for the Chesapeake Channel against observations from this study, subordinate station #4446 (labeled as "Cape Henry Light, 2 nm north of") was selected from NOAA's Tidal Current Tables (*e.g.* NOAA, 1995). This station was selected because it is coincident with the Chesapeake Channel's longitudinal axis. NOAA's (1999b) predicted tidal current speeds for this station at the published depths of 4.5 m, 11.8 m, and 16.4 m were compared to observations of maximum current speed from observations (Figure 4). This is one of the few Bay locations where information for three depths is provided in the Tables (NOAA, 1995). To develop a measure of accuracy for these predicted currents, a correlation coefficient (r) was determined by comparing current speed observations versus the predicted current speed using one of the three prediction depths which was closest to the observation depth. This approach yielded r = 0.79. Across-channel and depth variability could not be assessed because the information is not provided in the Tidal Current Tables.

The data analysis is for three data groups listed in Table 4. Figure 5 illustrates predictive curves based on the five data points of Group I. The data point at 0.0 relative hours repeats at 12.4 hours for mathematical continuity. Group II and III

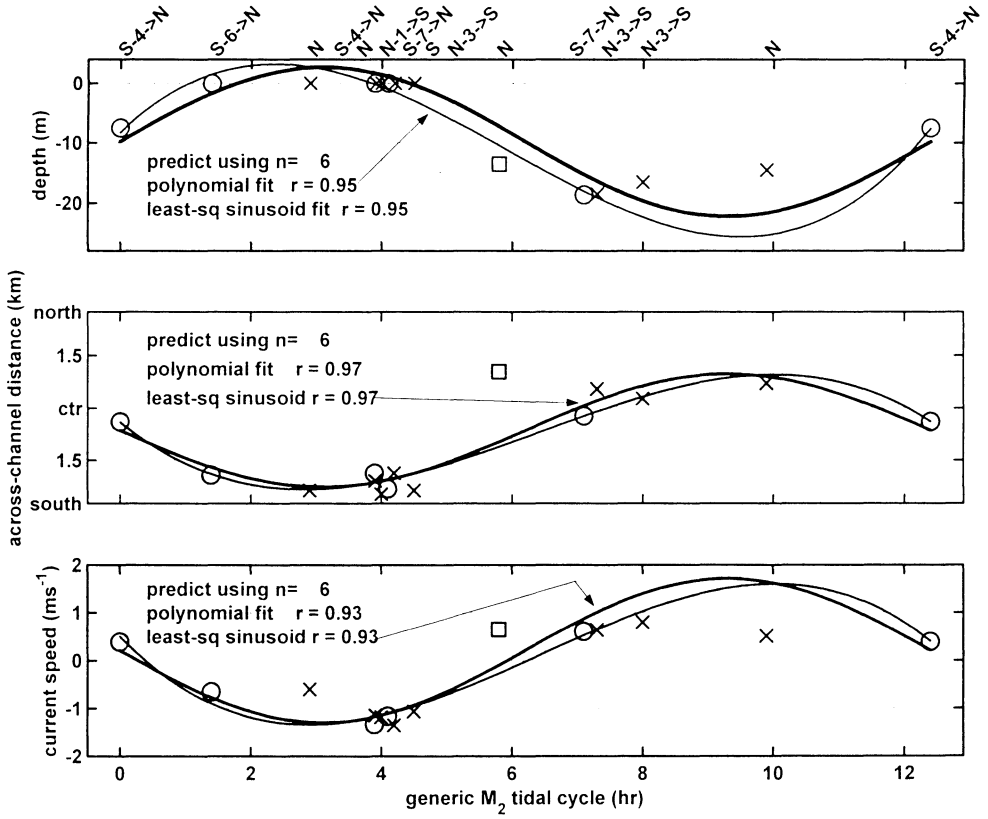

Figure 5. Polynomial (thin curve) and least-squares sinusoidal (thick curve) fit, based on Group I observations only, for the parameters of depth, across-channel location, and current speed of tidal current core maxima. Group I data are represented by circles. Remaining data are represented by x's with one outlier data represented by a box. Positive current speed correlates to a flood current. Across-channel center correlates to the across-channel center of the Chesapeake Channel. Correlation coefficients are designated by "r". Annotations at the top of the figure refer to the fortnightly tidal cycle, *e.g.* "S-4->N" indicates the data set was acquired four days after a spring tide.

data are also shown on Figure 5, but they were not used for the fit schemes. Both the polynomial and the sinusoidal fit for all three parameters have high correlation coefficients ($\geq$ 0.93) indicating strong positive correlation. Predictive algorithms and correlation coefficients are listed in Table 6. This first analysis shows that with only five data points, a reasonably good fit is achievable.

Curve fits were next determined by using all three Groups as one data set. The third and final analysis (Figure 6 and Table 6) was conducted using all three data sets minus transect #20–14 which appeared in Figures 5 and 6 as an outlier set of data at t = 5.8 hours. This analysis produced correlation coefficients for depth, across-channel location, and speed of 0.95, 0.97, and 0.93, respectfully, using both a least-squares sinusoidal and third degree polynomial fit when matched to observations. Using the polynomial fit, the range of error and mean error between prediction and observations for depth were: −2.9 m to 3.0 m/0.0 m; for across-channel location: −510 m to 380 m/< 1 m; and for speed: −0.58 ms^{-1} to 0.27 ms^{-1}/ <.001 ms^{-1}.

CONCLUSIONS

Comprehensive knowledge of tidal currents is important. Being able to predict the depth, across-channel location, and speed variability of tidal current core maxima is especially important.

Through an estuary mouth, tidal currents are highly variable in terms of depth, across-channel location, speed, and duration. They will often have jet maxima whose spatial and temporal characteristics are unknown. Even tidal current publications for one of the world's most studied estuaries, the Chesapeake Bay, do not provide this information. Most of the world's estuaries have limited to minimal tidal current prediction coverage.

This paper describes a simple, first-order, empirical method for making reasonable predictions of the depth, across-channel location, and speed variability of tidal current core maxima at the mouth of the Chesapeake Bay during summer months and in relatively steady state conditions of atmospheric forcing and freshwater input. It is based on making fourteen ADCP transects over a semidiurnal tidal cycle and fortnightly tidal range variation. This methodology is especially useful since no other method is available. Tidal current data from this experiment show strong periodicity in depth, across-channel location, and current speed related to the dominant tidal current harmonic constituent, M_2, and to a much lesser extent, to

Table 6. *Predictive algorithms and corresponding correlation coefficients (r) for depth, across-channel location, and current speed based on observations. "t" represents a generic tidal cycle measured in hours.*

Fit Scheme	Algorithms	r
	GROUP I OBSERVATIONS ONLY (n = 6)	
polynomial:	depth (m) = $0.16\ t^3 - 2.81\ t^2 + 10.61\ t - 8.22$	r = 0.95
lsq sinusoid:	depth (m) = $-9.76 + 12.46\ \sin([2\pi/12.4]\ t)$	r = 0.95
polynomial:	across (km) = $-0.02\ t^3 + 0.34\ t^2 - 1.51\ t - 0.40$	r = 0.97
lsq sinusoid:	across (km) = $-0.64 - 1.62\ \sin([2\pi/12.4]\ t)$	r = 0.97
polynomial:	speed (ms^{-1}) = $-0.02\ t^3 + 0.31\ t^2 - 1.41\ t + 0.50$	r = 0.93
lsq sinusoid:	speed (ms^{-1}) = $0.21 - 1.51\ \sin([2\pi/12.4]\ t)$	r = 0.93
	ALL OBSERVATIONS (n = 15)	
polynomial:	depth (m) = $0.12\ t^3 - 2.21\ t^2 + 8.37\ t - 7.16$	r = 0.95
lsq sinusoid:	depth (m) = $-9.45 + 10.38\ \sin([2\pi/12.4]\ t)$	r = 0.95
polynomial:	across (km) = $-0.02\ t^3 + 0.36\ t^2 - 1.51\ t - 0.51$	r = 0.97
lsq sinusoid:	across (km) = $-0.56 - 1.66\ \sin([2\pi/12.4]\ t)$	r = 0.97
polynomial:	speed (ms^{-1}) = $-0.01\ t^3 + 0.25\ t^2 - 1.15\ t + 0.40$	r = 0.93
lsq sinusoid:	speed (ms^{-1}) = $0.03 - 1.13\ \sin([2\pi/12.4]\ t)$	r = 0.93
	ALL OBSERVATIONS MINUS ONE OUTLIER (n = 14)	
polynomial:	depth (m) = $0.12\ t^3 - 2.21\ t^2 + 8.57\ t - 7.46$	r = 0.95
lsq sinusoid:	depth (m) = $-8.99 + 10.30\ \sin([2\pi/12.4]\ t)$	r = 0.95
polynomial:	across (km) = $-0.02\ t^3 + 0.36\ t^2 - 1.59\ t - 0.39$	r = 0.97
lsq sinusoid:	across (km) = $-0.71 - 1.63\ \sin([2\pi/12.4]\ t)$	r = 0.97
polynomial:	speed (ms^{-1}) = $-0.01\ t^3 + 0.25\ t^2 - 1.19\ t + 0.45$	r = 0.93
lsq sinusoid:	speed (ms^{-1}) = $-0.04 - 1.11\ \sin([2\pi/12.4]\ t)$	r = 0.93

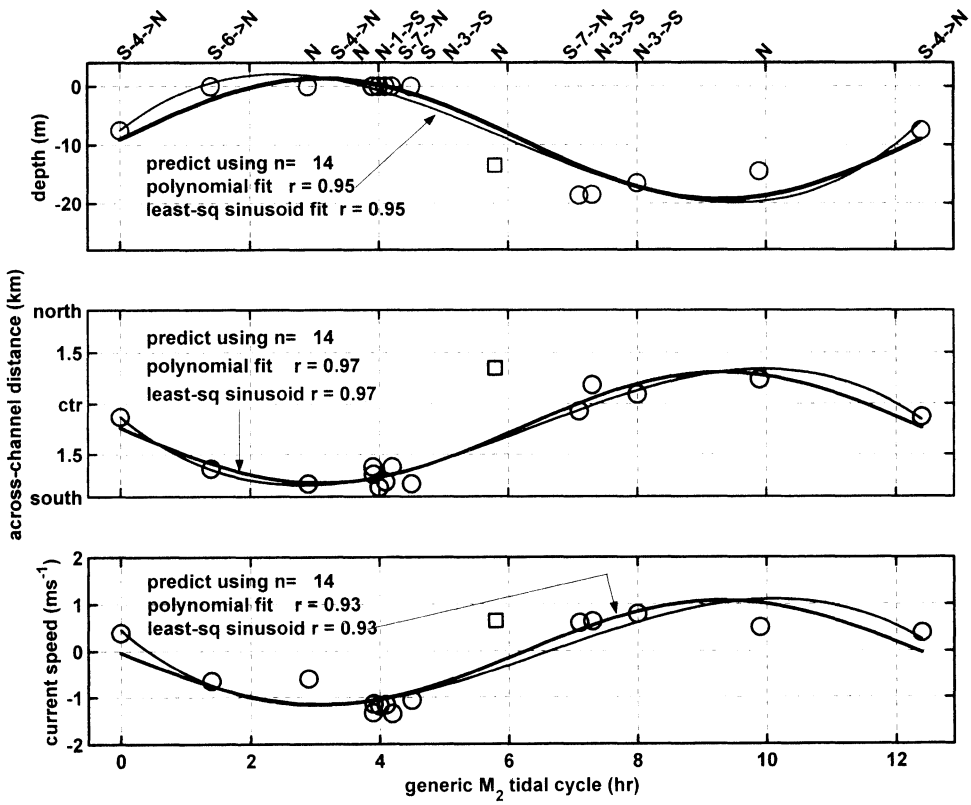

Figure 6. Polynomial (thin curve) and least-squares sinusoidal (thick curve) fit, based on all observations minus one outlier data set of transect #20–14, for the parameters of depth, across-channel location, and current speed of tidal current core maxima. All data minus the outlier are represented by circles. The one outlier data is represented with a box. Positive current speed correlates to a flood current. Across-channel center correlates to the across-channel center of the Chesapeake Channel. Correlation coefficients are designated by "r". Annotations at the top of the figure refer to the fortnightly tidal cycle, *e.g.* "S-4->N" indicates the data set was acquired four days after a spring tide.

the fortnightly variation of tidal range. The amplitude of the tidal range of these fourteen data sets extended from 0.564 m to 1.004 m, doubling from minimum to maximum. The observed and predictive results show that, even with this wide variability, correlation is very reasonable. In essence, the varying tidal range amplitude did not measurably affect the depth, across-channel location, or speed variability of the core. This variability is modeled in a least squares sense using both a sinusoidal function, related to the dominant tidal current harmonic constituent, and a third-degree polynomial curve fit. Prediction algorithms developed from both mathematical models predict variability in tidal current core maxima. Both prediction models produced correlation coefficients for depth, across-channel location, and speed of 0.95, 0.97, and 0.93, respectively. NOAA tidal current tables had a speed correlation coefficient of only 0.79 when matched to observations. Comparison correlation coefficients for depth and across-channel location from NOAA tidal current tables could not be determined since the tables do not provide depth and across-channel location information. Using the polynomial fit, the range of error and mean error between prediction and observations for depth were: −2.9 m to 3.0 m/0.0 m; for across-channel location: −510 m to 380 m/< 1 m; and for speed: -0.58 ms $^{-1}$ to 0.27 ms $^{-1}$/<.001 ms $^{-1}$. These models provide a simple, first-order, empirical means for predicting the depth, across-channel location, and speed variability of tidal current core maxima at the Chesapeake Bay mouth without long-term deployment of current meters at multiple depths and locations. Results were based on low wind and freshwater input conditions found in June and September. The procedure was not tested at other locations, nor under conditions of significant changes in freshwater input and wind. Algorithms developed would only apply under similar conditions of freshwater input and atmospheric forcing, and thus might only be valid on a seasonal basis. Algorithms would not be valid during extreme changes in environmental conditions such as storms and flooding. The procedure is not site specific. NOAA tidal current tables do not provide this detailed information. The procedure might be especially beneficial to estuaries where there are no tidal current meters or published tidal current information.

ACKNOWLEDGMENTS

Data collection was financed by the U.S. Naval Academy in support of midshipmen research. The author wishes to thank Mr. Doug Smith and Mr. Kenny Zepp for their technical assistance in ensuring all equipments were operational and in calibration, and the Craftmaster and crew of *YP 686* for their enthusiastic support during the cruise.

LITERATURE CITED

BOICOURT, W., 1981. Circulation in the Chesapeake Bay entrance region: Estuary-shelf interaction. *Chesapeake Bay Plume Study: Superflux 1980,* NASA Conference Publication 2188, 61–78.

BROWNE, D. R. and FISHER, C. W., 1988. Tide and Tidal Currents in the Chesapeake Bay. *NOAA Technical Report NOS OMA 3,* Rockville, MD, 84pp. plus appendices.

DOYLE, B.E. and WILSON, R.E., 1978. Lateral dynamic balance in the Sandy Hook to Rockaway Point transect. *Estuarine and Coastal Marine Science* 6, 165–174.

DYER, K. R., 1997. *Estuaries: a physical introduction.* New York: Wiley, 195p.

EHRET, W.T. and KENDRICK, T., 1999. Physical Oceanographer and Senior Physical Oceanographer, NOAA, National Ocean Service, Oceanographic Products and Services Division, User Services Branch, Silver Spring, MD. Written communication.

ELLIOTT, A. J., 1978. Observations of the meteorologically induced circulation in the Potomac Estuary. *Estuarine and Coastal Marine Science,* 6, 285–299.

FISHER, C.W., 1986. Tidal Circulation in Chesapeake Bay. Ph.D. Dissertation. Old Dominion University. Norfolk, Virginia, USA, 255 pp.

GOODRICH, D.M., 1987. Nontidal exchange processes at the Chesapeake Bay entrance. *Proceedings of the National Conference of Hydraulic Engineering,* (ASCE), Williamsburg, Virginia, USA, pp. 493–498.

LI, C. and VALLE-LEVINSON, A., 1999. A two-dimensional analytic tidal model for a narrow estuary of arbitrary lateral depth variation: The intratidal motion. *Journal of Geophysical Research,* 104, 23,525–23,543.

NOAA, U.S. Department of Commerce, 1995. *Tidal Current Tables 1996; Atlantic Coast of North America.* Silver Spring, Maryland, USA, 205p.

NOAA, U.S. Department of Commerce, 1997. *Product request provided by Coastal and Estuarine Oceanography Branch (N/OES23).* Silver Spring, Maryland, USA.

NOAA, U.S. Department of Commerce, 1999a. *Tidal Current Tables 2000; Atlantic Coast of North America.* Silver Spring, Maryland, USA, 213p.

NOAA, U.S. Department of Commerce, 1999b. *Product request provided by Coastal and Estuarine Oceanography Branch (N/OES23).* Silver Spring, Maryland, USA.

OFFICER, C. B., 1976. *Physical Oceanography of Estuaries and Associated Coastal Waters.* New York: Wiley, 465p.

ONG, J. E.; GONG, W. K., and UNCLES, R. J., 1994. Transverse structure of semi-diurnal currents over a cross-section of the Merbok Estuary, Malaysia. *Estuarine, Coastal and Shelf Science,* 38, 283–290.

OPEN UNIVERSITY COURSE TEAM, 1989. *Waves, Tides, and Shallow-water Processes.* Oxford UK: Pergamon, 187p.

PARASO, M. C. and VALLE-LEVINSON, A., 1996. Meteorological Influences on Sea Level and Water Temperature in the Lower Chesapeake Bay: 1992. *Estuaries,* 19, 548–561.

RD INSTRUMENTS, 1991. *Vessel Mounted Acoustic Doppler Current Profiler (VM-ADCP)* Technical Manual. San Diego California, USA, 170 pp.

RD INSTRUMENTS, 2000. Personal conversation and email correspondence with Mr. A.D. Johnson Jr., Field Service Engineer, Customer Service Group, RD Instruments, San Diego, California.

RICHARDS, D. and GRANAT, M., 1986. Salinity Redistributions in Deepened Estuaries. *In: Estuarine Variability,* WOLFE, D. A. (ed.), New York: Academic, pp 463–482.

SPIEGEL, M.R., 1975. *Probability and Statistics.* New York: McGraw-Hill, 260p.

VALLE-LEVINSON, A. and LWIZA, K. M. M., 1995. The effects of channels and shoals on exchange between the Chesapeake Bay and the adjacent ocean. *Journal of Geophysical Research,* 100, no. C9, 18,551–18,563.

VALLE-LEVINSON, A. and LWIZA, K. M. M., 1997. Bathymetric influences on the lower Chesapeake Bay hydrography. *Journal of Marine Systems,* 12, 221–236.

VALLE-LEVINSON, A.; LI, C.; ROYER, T.C., and ATKINSON, L.P., 1998. Flow patterns at the Chesapeake Bay entrance. *Continental Shelf Research,* 18, 1157–1177.

VALLE-LEVINSON, A.; LWIZA, K., and LI, C., 1999. Identifying Dirfferent Flow Constituents in Estuaries. *Circulation.* Center for Coastal Physical Oceanography, Old Dominion University, Norfolk VA, 1–2.

VENNELL, R., 1994. Acoustic Doppler Current Profiler measurements of tidal phase and amplitude in Cook Strait, New Zealand. *Continental Shelf Research* 14, 353–364.

WANG, D. P. and ELLIOTT, A. J., 1978. Nontidal variability in the Chesapeake Bay and Potomac River: evidence for nonlocal forcing. *Journal of Physical Oceanography,* 8, 225–232.

WANG, D. P., 1979. Subtidal sea level variations in Chesapeake Bay and relations to atmospheric forcing. *Journal of Physical Oceanography,* 9, 413–421.

WHITFORD, D. J., 1999. Observations of Current Flow Through the Mouth of the Chesapeake Bay. *Estuarine, Coastal and Shelf Science,* 49, 209–220.